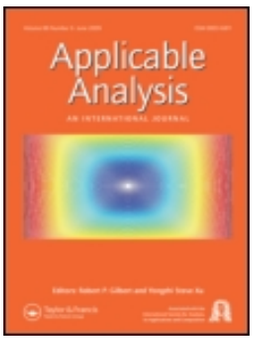

Taylor & Francis
Taylor & Francis Group

Applicable Analysis
An International Journal

ISSN: 0003-6811 (Print) 1563-504X (Online) Journal homepage: https://www.tandfonline.com/loi/gapa20

Convergence of adaptive FEM for some elliptic obstacle problem

M. Page & D. Praetorius

To cite this article: M. Page & D. Praetorius (2013) Convergence of adaptive FEM for some elliptic obstacle problem, Applicable Analysis, 92:3, 595-615, DOI: 10.1080/00036811.2011.631916

To link to this article: https://doi.org/10.1080/00036811.2011.631916

Applicable Analysis, 2013
Vol. 92, No. 3, 595–615, http://dx.doi.org/10.1080/00036811.2011.631916

Convergence of adaptive FEM for some elliptic obstacle problem

M. Page* and D. Praetorius

Institute for Analysis and Scientific Computing, Vienna UT, Wiedner Hauptstrasse 8-10, 1040 Vienna, Austria

Communicated by C. Bacuta

(*Received 23 August 2011; final version received 11 October 2011*)

In this work, we treat the convergence of adaptive lowest-order FEM for some elliptic obstacle problem with affine obstacle. For error estimation, we use a residual error estimator from [D. Braess, C. Carstensen, and R. Hoppe, *Convergence analysis of a conforming adaptive finite element method for an obstacle problem*, Numer. Math. 107 (2007), pp. 455–471]. We extend recent ideas from [J. Cascon, C. Kreuzer, R. Nochetto, and K. Siebert, *Quasi-optimal convergence rate for an adaptive finite element method*, SIAM J. Numer. Anal. 46 (2008), pp. 2524–2550] for the unrestricted variational problem to overcome the lack of Galerkin orthogonality. The main result states that an appropriately weighted sum of energy error, edge residuals and data oscillations satisfies a contraction property within each step of the adaptive feedback loop. This result is superior to a prior result from Braess et al. (2007) in two ways: first, it is unnecessary to control the decay of the data oscillations explicitly; second, our analysis avoids the use of some discrete local efficiency estimate so that the local mesh-refinement is fairly arbitrary.

Keywords: adaptive finite element methods; elliptic obstacle problems; convergence analysis

AMS Subject Classifications: 65N12; 65N30; 65N50; 65K15

1. Introduction

1.1. *Prior work on convergence of adaptive FEM*

Adaptive finite element methods for partial differential equations based on various types of *a posteriori* error estimators have been intensively studied and are now a standard tool in science and engineering (see, e.g. the monographs [1,2] and the references therein). As far as *a posteriori* error analysis for elliptic obstacle problems is concerned, we refer to [3–11].

In the case of elliptic boundary value problems, convergence of adaptive mesh-refining algorithms has first been proven in [12], followed by [13]. The latter works

*Corresponding author. Email: marcus.page@tuwien.ac.at

considered the residual error estimator for a P1-finite element discretization of the Poisson problem. In [13], the convergence analysis is based on reliability and the so-called *discrete local efficiency* of the residual error estimator, which relies on an *interior node property* for the local mesh-refinement. The main idea of the convergence proof then is to show that the error is contractive up to the data oscillations. This concept attracted quite some attention in the literature for various applications, e.g. the p-Laplacian [14], edge elements [15], mixed methods [16], nonconforming elements [17], and obstacle problems [18,19].

For the Poisson problem, optimality of the adaptive algorithm from [13] was first shown in [20]. Recently, Cascon et al. [21] presented a new convergence proof under weaker conditions. They showed that a weighted sum of error and error estimator satisfies a contraction property *without* requiring (discrete local) efficiency of the estimator. In particular, their proof avoided the interior node property of the local mesh-refinement, and they even proved optimality.

1.2. *Contributions of current work*

We consider the framework in [18], i.e. adaptive P1-finite elements for some elliptic obstacle problem with affine obstacle. The obstacle problem is a classic introductory example to study variational inequalities which represent a whole class of problems that often arise in physical and economical context. One major application is the oscillation of a membrane that must stay above a certain obstacle. Other examples are filtration in porous media or the Stefan problem (i.e. melting solids) (see, e.g. [22] and the references therein).

In order to explain the differences to [18], we first recall their main result: Let $\varepsilon_\ell = \mathcal{J}(U_\ell) - \mathcal{J}(u) \geq 0$ denote the energy error, where u is the exact solution of the obstacle problem and U_ℓ is the finite element approximation in the ℓ-th step of the adaptive algorithm. Based on a residual error estimator ϱ_ℓ consisting only of edge jumps and inspired by Morin et al. [13], Braess et al. [18, Theorem 3] states that the ϱ_ℓ-steered adaptive mesh-refinement leads to

$$\varepsilon_{\ell+1} \leq \kappa\, \varepsilon_\ell + C\, \mathrm{osc}_\ell^2 \quad \text{for all } \ell \in \mathbb{N}, \tag{1}$$

with osc_ℓ being the data oscillations (essentially across edges, cf (13)–(14) below) and with $0 < \kappa < 1$ and $C > 0$ being ℓ-independent constants. It is thus a consequence of elementary calculus that $\mathrm{osc}_\ell \to 0$ implies convergence $\varepsilon_\ell \to 0$ as $\ell \to \infty$. In [13,18], however, the convergence $\mathrm{osc}_\ell \to 0$ of the data oscillations has to be guaranteed by the implementation. This is usually done by performing additional local refinements until $\mathrm{osc}_{\ell+1}^2 \leq \vartheta\, \mathrm{osc}_\ell^2$ for some fixed constant $0 < \vartheta < 1$. We stress, however, that [18] provides no mathematical foundation on this step since the edge oscillations osc_ℓ are non-local. It is a technical byproduct of this work that edge oscillations satisfy a contraction property (Lemma 3.3), and thus the aforementioned algorithm from [18] is well-defined (cf Section 3.3).

Moreover, the main ingredients of the proof of (1) in [18] are the *reliability* of the error estimator, its *discrete local efficiency* and the *marking strategy* introduced by Dörfler [12] ensuring an appropriate selection of edges and elements for refinement. The *discrete local efficiency*, however, strongly relies on the *interior node property* of

the local mesh-refinement, and thus the validity of the convergence analysis is constrained by the refinement strategy.

We follow a different convergence approach, inspired by [21]: our main result (Theorem 3.4, Corollary 3.5) states that the adaptive algorithm steered by $\eta_\ell^2 = \varrho_\ell^2 + \operatorname{osc}_\ell^2$, i.e. steered by edge jumps plus data oscillations, leads to

$$\Delta_{\ell+1} \leq \kappa \Delta_\ell \quad \text{for all } \ell \in \mathbb{N}, \tag{2}$$

with a weighted sum $\Delta_\ell = \varepsilon_\ell + \gamma \eta_\ell^2$ and with $0 < \gamma$, $\kappa < 1$ being ℓ-independent constants. Note that the choice of our combined estimator has another advantage compared to [18]: from the linear case (cf [21, Section 6.2]), one knows that separate marking and refinement might lead to suboptimal convergence rates, whereas the combined marking strategy does not. Moreover, our result is fairly independent of the chosen mesh-refinement and does not need the *interior node property* as does the analysis in [18].

The first step for our proof of (2) is to show that the sequence of the estimators η_ℓ is contractive in the sense that

$$\eta_{\ell+1}^2 \leq q \eta_\ell^2 + C \left|\!\left|\!\left| U_{\ell+1} - U_\ell \right|\!\right|\!\right|^2 \quad \text{for all } \ell \in \mathbb{N}, \tag{3}$$

where $C > 0$ and $q \in (0, 1)$ are certain ℓ-independent constants and $|||\cdot|||$ denotes the energy norm (Proposition 3.1). To show this, we exploit the definition of the error estimator η_ℓ, the marking strategy used, and basic properties of the local mesh-refinement. In addition and contrary to [21], our elementary analysis avoids to dominate the data oscillations osc_ℓ by the element residuals $\|h_\ell f\|_{L^2(\Omega)}$ and is thus much more accurate if f is smooth but quantitatively large.

1.3. *Outline of current work*

In Section 2, we formulate the continuous and discrete obstacle problem, stated as energy minimization problems. Moreover, we recall the error estimator η_ℓ from [18] which is later on used to steer our adaptive algorithm, and state its reliability (Proposition 2.2). In Section 3.1, we recall the marking strategy and the local mesh-refinement used. As a consequence, we prove that the estimator η_ℓ satisfies an estimator reduction property (Proposition 3.1) (cf (3)). One major part of our proof is to show that the edge data oscillations are, in fact, contractive (Lemma 3.3). Finally, Section 3.2 states our version of the η_ℓ-steered adaptive mesh-refining algorithm (Algorithm 1) and proves the contraction result (2). In particular, the generated sequence of discrete solutions U_ℓ converges, in fact, to the continuous solution u (Theorem 3.4). A short Section 3.3 considers the algorithm of [18] and comments on improvements which are byproducts of our analysis (Theorem 3.8). A numerical experiment in Section 4 concludes this work.

2. Model problem

2.1. *Continuous formulation of model problem*

Let Ω be a bounded domain in $\mathbb{R}^2$ with polygonal boundary $\Gamma := \partial\Omega$. We define an obstacle on $\overline{\Omega}$ by the affine function χ with $\chi \leq 0$ on $\partial\Omega$. By $\mathcal{A} \subset H_0^1(\Omega)$,

we denote the set of admissible functions

$$\mathcal{A} = \big\{ v \in H^1_0(\Omega) \,:\, v \geq \chi \text{ a.e. in } \Omega \big\}, \tag{4}$$

which is convex, closed and non-empty. For given $f \in L^2(\Omega)$, we consider the energy functional

$$\mathcal{J}(v) = \frac{1}{2} \langle\!\langle v, v \rangle\!\rangle - \langle f, v \rangle, \tag{5}$$

where the energy scalar product reads

$$\langle\!\langle u, v \rangle\!\rangle = \int_\Omega \nabla u \cdot \nabla v \, \mathrm{d}x \quad \text{for all } u, v \in H^1_0(\Omega) \tag{6}$$

and where

$$\langle f, v \rangle = \int_\Omega f v \, \mathrm{d}x \tag{7}$$

denotes the L^2-scalar product. By $|||\cdot|||$, we denote the energy norm on $H^1_0(\Omega)$ induced by $\langle\!\langle \cdot, \cdot \rangle\!\rangle$. The minimization problem then reads as follows: *find $u \in \mathcal{A}$ such that*

$$\mathcal{J}(u) = \min_{v \in \mathcal{A}} \mathcal{J}(v). \tag{8}$$

The following well-known abstract lemma, found e.g. in [23, Theorem II.2.1], states unique solvability of this problem and equivalence to some variational inequality.

LEMMA 2.1 *Let $\mathcal{H}$ be a Hilbert space over $\mathbb{R}$ with scalar product $\langle\!\langle \cdot, \cdot \rangle\!\rangle$ and induced norm $|||\cdot|||$. For any closed, convex and non-empty subset $\mathcal{A}$ of $\mathcal{H}$ and any linear functional $f \in \mathcal{H}^*$, there is a unique minimizer $u \in \mathcal{A}$ of* (8). *This minimizer is equivalently characterized in terms of the following variational inequality*: *find $u \in \mathcal{A}$ such that*

$$\langle\!\langle u, u - v \rangle\!\rangle \leq f(u - v) \tag{9}$$

for all $v \in \mathcal{A}$.

2.2. *Conforming discretization*

For the numerical solution of (8), we consider conforming and shape regular triangulations $\mathcal{T}_\ell$ of Ω and denote the standard P1-finite element space of globally continuous and piecewise affine functions by $\mathcal{S}^1(\mathcal{T}_\ell)$. The finite-dimensional minimization problem then reads as follows: *find $U_\ell \in \mathcal{A}_\ell := \mathcal{A} \cap \mathcal{S}^1(\mathcal{T}_\ell)$ such that*

$$\mathcal{J}(U_\ell) = \min_{V_\ell \in \mathcal{A}} \mathcal{J}(V_\ell). \tag{10}$$

Note that $\mathcal{A}_\ell$ is a non-empty, convex and closed subset of $\mathcal{S}^1(\mathcal{T}_\ell)$. With the same arguments as for the continuous problem, (10) admits a unique solution $U_\ell \in \mathcal{A}_\ell$.

Throughout all sections, the set of all interior edges $E = T^+ \cap T^-$ for certain elements T^+, $T^- \in \mathcal{T}_\ell$ is denoted by $\mathcal{E}_\ell$. The set of all edges of $\mathcal{T}_\ell$ is denoted by $\mathcal{E}_\ell^\star$. In particular, $\mathcal{E}_{\ell,\Gamma} := \mathcal{E}_\ell^\star \backslash \mathcal{E}_\ell$ contains all boundary edges and provides some partition of Γ.

2.3. *Reliable error estimator*

Now, let $u \in \mathcal{A}$ denote the continuous solution of (8) and $U_\ell \in \mathcal{A}_\ell$ be the discrete solution of (10) for some fixed triangulation $\mathcal{T}_\ell$. To steer the adaptive mesh-refinement, we use some residual-based error estimator

$$\eta_\ell^2 := \varrho_\ell^2 + \operatorname{osc}_\ell^2 \quad \text{with} \quad \varrho_\ell^2 = \sum_{E \in \mathcal{E}_\ell} \varrho_\ell(E)^2 \quad \text{and} \quad \operatorname{osc}_\ell^2 = \sum_{E \in \mathcal{E}_\ell^\star} \operatorname{osc}_\ell(E)^2 \tag{11}$$

from [18]: first, $\varrho_\ell(E)^2$ denotes the weighted L^2-norms of the normal jump

$$\varrho_\ell(E)^2 := h_E \, \|[\partial_n U_\ell]\|_{L^2(E)}^2 \quad \text{for } E \in \mathcal{E}_\ell \tag{12}$$

with $h_E = \operatorname{diam}(E)$ the length of E and $[\cdot]$ the jump over an interior edge $E = T^+ \cap T^- \in \mathcal{E}_\ell$. Second, $\operatorname{osc}_\ell(E)^2$ denotes the data oscillations of f over E

$$\operatorname{osc}_\ell(E)^2 := |\Omega_{\ell,E}| \, \| f - f_{\Omega_{\ell E}} \|_{L^2(\Omega_{\ell,E})}^2 \quad \text{for } E \in \mathcal{E}_\ell \tag{13}$$

with $\Omega_{\ell,E} = T^+ \cup T^-$ the patch associated with E and $f_{\Omega_{\ell E}} = (1/|\Omega_{\ell,E}|) \int_{\Omega_{\ell E}} f \, \mathrm{d}x$ the corresponding integral mean of f. Finally, for edges E on the boundary, η_ℓ involves the weighted element residuals

$$\operatorname{osc}_\ell(E)^2 := |T| \|f\|_{L^2(T)}^2 \quad \text{for } E \in \mathcal{E}_{\ell,\Gamma}, \tag{14}$$

where $T \in \mathcal{T}_\ell$ is the unique element with $E = \partial T \cap \Gamma$. The following proposition has essentially been shown in [18], where $\operatorname{osc}_\ell(E)$ for boundary edges $E \in \mathcal{E}_{\ell,\Gamma}$ is, however, weighted by $\operatorname{diam}(T)^2 \sim |T|$. We will discuss this, up to shape regularity, equivalent definition later on (cf Corollary 3.5 in Section 3.2).

Proposition 2.2 *The estimator η_ℓ from* (11) *is reliable in the sense that there holds*

$$\frac{1}{2} \, |\!|\!| u - U_\ell |\!|\!|^2 \le \mathcal{J}(U_\ell) - \mathcal{J}(u) \le C_1 \, \eta_\ell^2. \tag{15}$$

The constant $C_1 > 0$ depends only on Ω and the shape of the elements in $\mathcal{T}_\ell$.

Proof The upper bound is stated in [18, Theorem 1] and hinges on the fact that the obstacle is affine. To see the lower bound, we use the variational inequality (9). For $v = U_\ell$, this gives

$$\begin{aligned} |\!|\!| u - U_\ell |\!|\!|^2 &= \langle\!\langle u, u - U_\ell \rangle\!\rangle + |\!|\!| U_\ell |\!|\!|^2 - \langle\!\langle U_\ell, u \rangle\!\rangle \\ &\le \left(\frac{1}{2} \, |\!|\!| U_\ell |\!|\!|^2 - \langle f, U_\ell \rangle \right) - \left(\frac{1}{2} \, |\!|\!| u |\!|\!|^2 - \langle f, u \rangle \right) \\ &\quad + \left(\frac{1}{2} \, |\!|\!| U_\ell |\!|\!|^2 - \langle\!\langle U_\ell, u \rangle\!\rangle + \frac{1}{2} \, |\!|\!| u |\!|\!|^2 \right) \\ &= \mathcal{J}(U_\ell) - \mathcal{J}(u) + \frac{1}{2} \, |\!|\!| u - U_\ell |\!|\!|^2 \end{aligned}$$

and concludes the proof. ∎

Remark 1 Before proceeding we want to comment quickly on other error estimators for obstacle problems in the literature. In some works (see, e.g. [7,10], estimators that only contribute within the non-contact set are used. This has some

advantages since, for example, obstacles with kinks can be treated. The analysis in this case, however, becomes much more involved. In particular, it is unclear how to show an estimator reduction, or a contraction property in the sense of Proposition 3.1 or Theorem 3.4, respectively. As a consequence, for those kinds of estimators, only a weaker convergence result [10] can be shown, but not a contraction which is a crucial ingredient for a possible optimality analysis.

3. A convergent adaptive algorithm

3.1. *Estimator reduction*

As usual, we employ the local contributions of η_ℓ from (12)–(14) to steer the adaptive algorithm. For marking, we use the marking strategy introduced by Dörfler [12]. Contrary to [12,13,18], we mark simultaneously for $\varrho_\ell(E)$ and data oscillations $\operatorname{osc}_\ell(E)$: given some parameter $\theta \in (0,1)$, we seek a set $\mathcal{M}_\ell \subseteq \mathcal{E}_\ell^\star$ of usually minimal cardinality such that

$$\theta\,\eta_\ell^2 \le \sum_{E\in\mathcal{M}_\ell} \eta_\ell(E)^2 \quad \text{where} \quad \eta_\ell(E)^2 = \begin{cases} \varrho_\ell(E)^2 + \operatorname{osc}_\ell(E)^2 & \text{for } E \in \mathcal{E}_\ell \\ \operatorname{osc}_\ell(E)^2 & \text{for } E \in \mathcal{E}_{\ell,\Gamma}. \end{cases} \tag{16}$$

For the mesh-refinement, we use newest-vertex bisection, where we mark all edges $E \in \mathcal{M}_\ell$ for refinement. The refinement rules are shown in Figure 1, and the reader is also referred to [1, Chapter 4]. Besides uniform shape regularity of $\mathcal{T}_{\ell+1}$, there is a certain decay of the mesh-widths:

- Marked edges $E \in \mathcal{M}_\ell$ are split into two edges $E', E'' \in \mathcal{E}_{\ell+1}^\star$ of half length.
- If at least one edge E of an element $T \in \mathcal{T}_\ell$ is marked, T is refined into up to four son elements $T' \in \mathcal{T}_{\ell+1}$ with $|T|/4 \le |T'| \le |T|/2$ (cf Figure 1).

These observations are essential to prove the following result.

PROPOSITION 3.1 *Suppose that the set $\mathcal{M}_\ell \subseteq \mathcal{E}_\ell^\star$ satisfies* (16) *and marked edges are refined as stated before. Then, there holds*

$$\eta_{\ell+1}^2 \le q\,\eta_\ell^2 + C_2 |\!|\!| U_{\ell+1} - U_\ell |\!|\!|^2 \tag{17}$$

with some contraction constant $q \in (0,1)$ which depends only on $\theta \in (0,1)$. The constant $C_2 > 0$ additionally depends on the shape of the elements in $\mathcal{T}_0$.

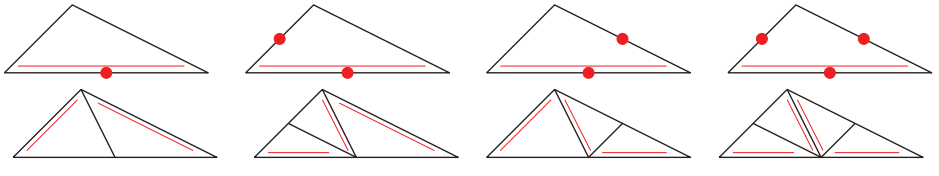

Figure 1. For each triangle $T \in \mathcal{T}$, there is one fixed *reference edge*, indicated by the double line (left, top). Refinement of T is done by bisecting the reference edge, where its midpoint becomes a new node. The reference edges of the son triangles are opposite to this newest vertex (left, bottom). To avoid hanging nodes, one proceeds as follows: we assume that certain edges of T, but at least the reference edge, are marked for refinement (top). Using iterated newest vertex bisection, the element is then split into 2, 3 or 4 son triangles (bottom).

For the convenience of the reader, the proof of Proposition 3.1 is split into two lemmas which estimate the decay of the different contributions of η_ℓ if the mesh $\mathcal{T}_\ell$ is locally refined.

LEMMA 3.2 *According to the refinement of marked edges $E \in \mathcal{E}_\ell \cap \mathcal{M}_\ell$, there holds*

$$\sum_{E' \in \mathcal{E}_{\ell+1}} h_{E'} \, \|[\partial_n U_\ell]\|^2_{L^2(E')} \leq \sum_{E \in \mathcal{E}_\ell} \varrho_\ell(E)^2 - \frac{1}{2} \sum_{E \in \mathcal{E}_\ell \cap \mathcal{M}_\ell} \varrho_\ell(E)^2. \tag{18}$$

Proof We define the set $\overline{\mathcal{M}}_{\mathcal{E},\ell} := \{E' \in \mathcal{E}_{\ell+1} : \exists E \in \mathcal{E}_\ell \cap \mathcal{M}_\ell \quad E' \subseteq E\}$ containing all edges obtained by refinement of marked edges. Then, one observes

$$\begin{aligned}
\sum_{E' \in \mathcal{E}_{\ell+1}} h_{E'} \, \|[\partial_n U_\ell]\|^2_{L^2(E')} &= \sum_{E' \in \mathcal{E}_{\ell+1} \backslash \overline{\mathcal{M}}_{\mathcal{E},\ell}} h_{E'} \, \|[\partial_n U_\ell]\|^2_{L^2(E')} + \sum_{E' \in \overline{\mathcal{M}}_{\mathcal{E},\ell}} h_{E'} \, \|[\partial_n U_\ell]\|^2_{L^2(E')} \\
&\leq \sum_{E \in \mathcal{E}_\ell \backslash \mathcal{M}_\ell} h_E \, \|[\partial_n U_\ell]\|^2_{L^2(E)} + \frac{1}{2} \sum_{E \in \mathcal{E}_\ell \cap \mathcal{M}_\ell} h_E \, \|[\partial_n U_\ell]\|^2_{L^2(E)} \\
&= \sum_{E \in \mathcal{E}_\ell \backslash \mathcal{M}_\ell} \varrho_\ell(E)^2 + \frac{1}{2} \sum_{E \in \mathcal{E}_\ell \cap \mathcal{M}_\ell} \varrho_\ell(E)^2,
\end{aligned}$$

where we have used that the jump $[\partial_n U_\ell]$ is zero on all edges $E' \in \mathcal{E}_{\ell+1}$ which lie inside an element $T \in \mathcal{T}_\ell$. ■

LEMMA 3.3 *Suppose that $\mathcal{T}_{\ell+1}$ is obtained by newest vertex bisection of $\mathcal{T}_\ell$. Then, independent of the set of marked edges, it holds that*

$$\operatorname{osc}^2_{\ell+1} \leq \operatorname{osc}^2_\ell - \frac{1}{4} \sum_{E \in \mathcal{E}^\star_\ell \backslash \mathcal{E}^\star_{\ell+1}} \operatorname{osc}_\ell(E)^2 \leq \operatorname{osc}^2_\ell. \tag{19}$$

Proof The proof of (19) is considerably longer than for the prior contributions in (18). The reason is that local mesh-refinement leads to additional edges inside the refined elements $T \in \mathcal{T}_\ell$. This provides additional contributions to $\operatorname{osc}_{\ell+1}$, which have to be controlled. For each edge $E \in \mathcal{E}^\star_{\ell+1}$ and each element $T \in \mathcal{T}_\ell$ with $|T \cap \Omega_{\ell+1,E}| > 0$, we define the quantity

$$\operatorname{osc}_{\ell+1}(E|T)^2 = |\Omega_{\ell+1,E}| \, \| f - f_{\Omega_{\ell+1},E} \|^2_{L^2(\Omega_{\ell+1,E} \cap T)}.$$

For a boundary edge $E \in \mathcal{E}_{\ell+1,\Gamma} = \mathcal{E}^\star_{\ell+1} \backslash \mathcal{E}_{\ell+1}$, this definition is understood with $\Omega_{\ell+1,E} := T'$ and $f_{\Omega_{\ell+1E}} := 0$, where $T' \in \mathcal{T}_{\ell+1}$ is the unique element with $E = \partial T' \cap \Gamma$. Throughout the proof, $f_\omega = (1/|\omega|) \int_\omega f \, \mathrm{d}x$ denotes the integral mean of f over the measurable set ω. Note that the L^2-best approximation property of f_ω yields

$$\| f - f_\omega \|_{L^2(\omega)} \leq \| f - \alpha \|_{L^2(\omega)} \quad \text{for all } \alpha \in \mathbb{R},$$

whence

$$\| f - f_\omega \|_{L^2(\omega)} \leq \| f - f_{\widehat{\omega}} \|_{L^2(\widehat{\omega})} \quad \text{for all measurable sets } \widehat{\omega} \supset \omega.$$

For each element $A \in \mathcal{T}_\ell$, only four cases occur: A is either not refined, i.e. $A \in \mathcal{T}_\ell \cap \mathcal{T}_{\ell+1}$, or refined by either one, two or three bisections (cf Figure 2).

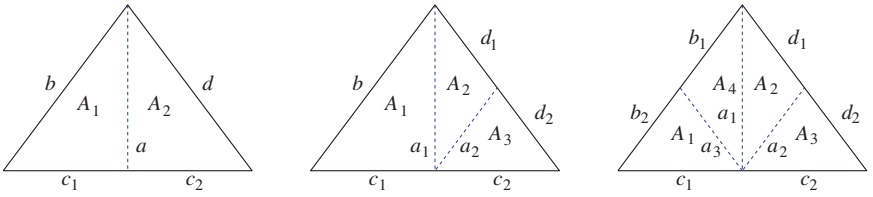

Figure 2. Refinement of an element A by one (a), two (b) or three (c) bisections and notation used in the proof of Lemma 3.3.

First, assume that an element $A \in \mathcal{T}_\ell \cap \mathcal{T}_{\ell+1}$ is not refined. Let $b, c, d \in \mathcal{E}_\ell \cap \mathcal{E}_{\ell+1}$ denote its three edges. We then define

$$o_\ell(b|A)^2 = \operatorname{osc}_{\ell+1}(b|A)^2, \quad o_\ell(c|A)^2 = \operatorname{osc}_{\ell+1}(c|A)^2, \quad \text{and} \quad o_\ell(d|A)^2 = \operatorname{osc}_{\ell+1}(d|A)^2.$$

By definition, we obtain

$$\sum_{\substack{E \in \mathcal{E}_{\ell+1}^\star \\ |A \cap \Omega_{\ell+1,E}| > 0}} \operatorname{osc}_{\ell+1}(E|A)^2 \le \sum_{\substack{E \in \mathcal{E}_\ell^\star \\ E \subset \partial A}} o_\ell(E|A)^2 \tag{20}$$

even with equality.

Second, assume that an element $A \in \mathcal{T}_\ell$ with edges $b, c, d \in \mathcal{E}_\ell^\star$ is refined by one bisection (cf Figure 2), where the edge c is split into $c_1, c_2 \in \mathcal{E}_{\ell+1}^\star$ and one additional edge $a \in \mathcal{E}_{\ell+1}^\star$ is created. Moreover, A is split into elements $A_1, A_2 \in \mathcal{T}_{\ell+1}$ with area $|A_1| = |A_2| = |A|/2$. Let $B, C, D \in \mathcal{T}_\ell$ be the neighbours of A along the edges $b, c, d \in \mathcal{E}_\ell^\star$, where for instance $B = \emptyset$ if $b \in \mathcal{E}_\ell^\star \backslash \mathcal{E}_\ell$ is a boundary edge. Then,

$$\begin{aligned}
&\sum_{\substack{E \in \mathcal{E}_{\ell+1}^\star \\ |A \cap \Omega_{\ell+1,E}| > 0}} \operatorname{osc}_{\ell+1}(E|A)^2 \\
&\quad = \operatorname{osc}_{\ell+1}(c_1|A)^2 + \operatorname{osc}_{\ell+1}(c_2|A)^2 + \operatorname{osc}_{\ell+1}(b|A)^2 + \operatorname{osc}_{\ell+1}(d|A)^2 + \operatorname{osc}_{\ell+1}(a|A)^2 \\
&\quad = \big(|\Omega_{\ell+1,c_1} \cap C| + |A|/2\big)\, \|f - f_{\Omega_{\ell+1,c_1}}\|_{L^2(A_1)}^2 + \big(|\Omega_{\ell+1,c_2} \cap C| + |A|/2\big)\, \|f - f_{\Omega_{\ell+1,c_2}}\|_{L^2(A_2)}^2 \\
&\qquad + \big(|\Omega_{\ell+1,b} \cap B| + |A|/2\big)\, \|f - f_{\Omega_{\ell+1,b}}\|_{L^2(A_1)}^2 + \big(|\Omega_{\ell+1,d} \cap D| + |A|/2\big)\, \|f - f_{\Omega_{\ell+1,d}}\|_{L^2(A_2)}^2 \\
&\qquad + |A|\, \|f - f_A\|_{L^2(A)}^2.
\end{aligned}$$

The last term belongs to the new edge $a \in \mathcal{E}_{\ell+1}^\star$. We define

$$\begin{aligned}
o_\ell(b|A)^2 &= \big(|\Omega_{\ell+1,b} \cap B| + |A|/2\big)\, \|f - f_{\Omega_{\ell+1,b}}\|_{L^2(A_1)}^2 + (|A|/2)\, \|f - f_A\|_{L^2(A)}^2, \\
o_\ell(c|A)^2 &= \big(|\Omega_{\ell+1,c_1} \cap C| + |A|/2\big)\, \|f - f_{\Omega_{\ell+1,c_1}}\|_{L^2(A_1)}^2 \\
&\qquad + \big(|\Omega_{\ell+1,c_2} \cap C| + |A|/2\big)\, \|f - f_{\Omega_{\ell+1,c_2}}\|_{L^2(A_2)}^2, \\
o_\ell(d|A)^2 &= \big(|\Omega_{\ell+1,d} \cap D| + |A|/2\big)\, \|f - f_{\Omega_{\ell+1,d}}\|_{L^2(A_2)}^2 + (|A|/2)\, \|f - f_A\|_{L^2(A)}^2
\end{aligned}$$

and observe that, by definition, (20) holds with equality.

Third, assume that an element $A \in \mathcal{T}_\ell$ with edges $b, c, d \in \mathcal{E}_\ell^\star$ is refined by two bisections (cf Figure 2), where the edges c, d are split into $c_1, c_2, d_1, d_2 \in \mathcal{E}_{\ell+1}^\star$, respectively, and two new edges $a_1, a_2 \in \mathcal{E}_{\ell+1}^\star$ are created. Moreover, A is split into

elements A_1, A_2, $A_3 \in \mathcal{T}_{\ell+1}$ with area $|A_1| = |A|/2$ and $|A_2| = |A_3| = |A|/4$. Let b, c, d and B, C, D be the same as in the previous case. Then,

$$\begin{aligned}
&\sum_{\substack{E\in\mathcal{E}^\star_{\ell+1}\\ |A\cap\Omega_{\ell+1,E}|>0}} \operatorname{osc}_{\ell+1}(E|A)^2\\
&\quad= \operatorname{osc}_{\ell+1}(c_1|A)^2 + \operatorname{osc}_{\ell+1}(c_2|A)^2 + \operatorname{osc}_{\ell+1}(d_1|A)^2 + \operatorname{osc}_{\ell+1}(d_2|A)^2 + \operatorname{osc}_{\ell+1}(b|A)^2\\
&\qquad + \operatorname{osc}_{\ell+1}(a_1|A)^2 + \operatorname{osc}_{\ell+1}(a_2|A)^2\\
&\quad= \big(|\Omega_{\ell+1,c_1}\cap C| + |A|/2\big)\,\|f-f_{\Omega_{\ell+1,c_1}}\|^2_{L^2(A_1)} + \big(|\Omega_{\ell+1,c_2}\cap C| + |A|/4\big)\,\|f-f_{\Omega_{\ell+1,c_2}}\|^2_{L^2(A_3)}\\
&\qquad + \big(|\Omega_{\ell+1,d_1}\cap D| + |A|/4\big)\,\|f-f_{\Omega_{\ell+1,d_1}}\|^2_{L^2(A_2)} + \big(|\Omega_{\ell+1,d_2}\cap D| + |A|/4\big)\\
&\qquad \times \|f-f_{\Omega_{\ell+1,d_2}}\|^2_{L^2(A_3)} + \big(|\Omega_{\ell+1,b}\cap B| + |A|/2\big)\,\|f-f_{\Omega_{\ell+1,b}}\|^2_{L^2(A_1)}\\
&\qquad + (3|A|/4)\,\|f-f_{A_1\cup A_2}\|^2_{L^2(A_1\cup A_2)} + (|A|/2)\,\|f-f_{A_2\cup A_3}\|^2_{L^2(A_2\cup A_3)}.
\end{aligned}$$

The last two terms belong to the new edges $a_1, a_2 \in \mathcal{E}^\star_{\ell+1}$ and are roughly estimated by

$$(3|A|/4)\,\|f-f_{A_1\cup A_2}\|^2_{L^2(A_1\cup A_2)} + (|A|/2)\,\|f-f_{A_2\cup A_3}\|^2_{L^2(A_2\cup A_3)} \le (5|A|/4)\,\|f-f_A\|^2_{L^2(A)}.$$

We define

$$\begin{aligned}
o_\ell(b|A)^2 &= \big(|\Omega_{\ell+1,b}\cap B| + |A|/2\big)\,\|f-f_{\Omega_{\ell+1,b}}\|^2_{L^2(A_1)} + (|A|/2)\,\|f-f_A\|^2_{L^2(A)},\\
o_\ell(c|A)^2 &= \big(|\Omega_{\ell+1,c_1}\cap C| + |A|/2\big)\,\|f-f_{\Omega_{\ell+1,c_1}}\|^2_{L^2(A_1)}\\
&\qquad + \big(|\Omega_{\ell+1,c_2}\cap C| + |A|/4\big)\,\|f-f_{\Omega_{\ell+1,c_2}}\|^2_{L^2(A_3)} + (|A|/4)\,\|f-f_A\|^2_{L^2(A)},\\
o_\ell(d|A)^2 &= \big(|\Omega_{\ell+1,d_1}\cap D| + |A|/4\big)\,\|f-f_{\Omega_{\ell+1,d_1}}\|^2_{L^2(A_2)}\\
&\qquad + \big(|\Omega_{\ell+1,d_2}\cap D| + |A|/4\big)\,\|f-f_{\Omega_{\ell+1,d_2}}\|^2_{L^2(A_3)} + (|A|/2)\,\|f-f_A\|^2_{L^2(A)}.
\end{aligned}$$

By definition, we again obtain (20).

Fourth, assume that an element $A \in \mathcal{T}_\ell$ with edges $b, c, d \in \mathcal{E}^\star_\ell$ is refined by three bisections (cf Figure 2), where the edges b, c, d are split into $b_1, b_2, c_1, c_2, d_1, d_2 \in \mathcal{E}^\star_{\ell+1}$, respectively, and three new edges $a_1, a_2, a_3 \in \mathcal{E}^\star_{\ell+1}$ are created. Moreover, A is split into elements $A_1, A_2, A_3, A_4 \in \mathcal{T}_{\ell+1}$ with area $|A_j| = |A|/4$. For b, c, d and B, C, D, we use the notation from the previous cases. Then,

$$\begin{aligned}
&\sum_{\substack{E\in\mathcal{E}^\star_{\ell+1}\\ |A\cap\Omega_{\ell+1,E}|>0}} \operatorname{osc}_{\ell+1}(E|A)^2\\
&\quad= \operatorname{osc}_{\ell+1}(b_1|A)^2 + \operatorname{osc}_{\ell+1}(b_2|A)^2 + \operatorname{osc}_{\ell+1}(c_1|A)^2 + \operatorname{osc}_{\ell+1}(c_2|A)^2\\
&\qquad + \operatorname{osc}_{\ell+1}(d_1|A)^2 + \operatorname{osc}_{\ell+1}(d_2|A)^2 + \operatorname{osc}_{\ell+1}(a_1|A)^2 + \operatorname{osc}_{\ell+1}(a_2|A)^2 + \operatorname{osc}_{\ell+1}(a_3|A)^2\\
&\quad\le \big(|\Omega_{\ell+1,b_1}\cap B| + |A|/4\big)\,\|f-f_{\Omega_{\ell+1,b_1}}\|^2_{L^2(A_4)} + \big(|\Omega_{\ell+1,b_2}\cap B| + |A|/4\big)\,\|f-f_{\Omega_{\ell+1,b_2}}\|^2_{L^2(A_1)}\\
&\qquad + \big(|\Omega_{\ell+1,c_1}\cap C| + |A|/4\big)\,\|f-f_{\Omega_{\ell+1,c_1}}\|^2_{L^2(A_1)} + \big(|\Omega_{\ell+1,c_2}\cap C| + |A|/4\big)\\
&\qquad \times \|f-f_{\Omega_{\ell+1,c_2}}\|^2_{L^2(A_3)} + \big(|\Omega_{\ell+1,d_1}\cap D| + |A|/4\big)\,\|f-f_{\Omega_{\ell+1,d_1}}\|^2_{L^2(A_2)}\\
&\qquad + \big(|\Omega_{\ell+1,d_2}\cap D| + |A|/4\big)\,\|f-f_{\Omega_{\ell+1,d_2}}\|^2_{L^2(A_3)} + (3|A|/2)\,\|f-f_A\|^2_{L^2(A)}.
\end{aligned}$$

Defining

$$\begin{aligned}
o_\ell(b|A)^2 &= \big(|\Omega_{\ell+1,b_1}\cap B| + |A|/4\big)\,\|f-f_{\Omega_{\ell+1b_1}}\|^2_{L^2(A_4)}\\
&\quad + \big(|\Omega_{\ell+1,b_2}\cap B| + |A|/4\big)\,\|f-f_{\Omega_{\ell+1b_2}}\|^2_{L^2(A_1)} + (|A|/2)\,\|f-f_A\|^2_{L^2(A)}\\
o_\ell(c|A)^2 &= \big(|\Omega_{\ell+1,c_1}\cap C| + |A|/4\big)\,\|f-f_{\Omega_{\ell+1c_1}}\|^2_{L^2(A_1)}\\
&\quad + \big(|\Omega_{\ell+1,c_2}\cap C| + |A|/4\big)\,\|f-f_{\Omega_{\ell+1c_2}}\|^2_{L^2(A_3)} + (|A|/2)\,\|f-f_A\|^2_{L^2(A)}\\
o_\ell(d|A)^2 &= \big(|\Omega_{\ell+1,d_1}\cap D| + |A|/4\big)\,\|f-f_{\Omega_{\ell+1d_1}}\|^2_{L^2(A_2)}\\
&\quad + \big(|\Omega_{\ell+1,d_2}\cap D| + |A|/4\big)\,\|f-f_{\Omega_{\ell+1d_2}}\|^2_{L^2(A_3)} + (|A|/2)\,\|f-f_A\|^2_{L^2(A)},
\end{aligned}$$

we again guarantee (20).

Now, it only remains to show that for non-refined edges holds

$$\sum_{\substack{T\in\mathcal{T}_\ell\\ T\subset\Omega_{\ell,E}}} o_\ell(E|T)^2 \le \operatorname{osc}_\ell(E)^2 \quad \text{for all } E\in\mathcal{E}_\ell^\star\cap\mathcal{E}_{\ell+1}^\star, \tag{21}$$

whereas for edges which are refined, there holds

$$\sum_{\substack{T\in\mathcal{T}_\ell\\ T\subset\Omega_{\ell,E}}} o_\ell(E|T)^2 \le \frac{3}{4}\operatorname{osc}_\ell(E)^2 \quad \text{for all } E\in\mathcal{E}_\ell^\star\backslash\mathcal{E}_{\ell+1}^\star. \tag{22}$$

Of course, there are quite some cases to be considered. Since all follow by direct calculation, we only consider some particular examples shown in Figure 3, while we refer to [24, Lemma 3.3.6] for the consideration of all possible cases.

We first consider $b := A\cap B\in\mathcal{E}_\ell$. According to our definitions, there holds

$$\begin{aligned}
o_\ell(b|B)^2 &= (|A|/2+|B|)\,\|f-f_{A_1\cup B}\|^2_{L^2(B)},\\
o_\ell(b|A)^2 &= (|B|+|A|/2)\,\|f-f_{A_1\cup B}\|^2_{L^2(A_1)} + (|A|/2)\,\|f-f_A\|^2_{L^2(A)}.
\end{aligned}$$

This implies

$$\begin{aligned}
o_\ell(b|A)^2 + o_\ell(b|B)^2 &= (|A|/2+|B|)\,\|f-f_{A_1\cup B}\|^2_{L^2(A_1\cup B)} + (|A|/2)\,\|f-f_A\|^2_{L^2(A)}\\
&\le (|A|/2+|B|)\,\|f-f_{A\cup B}\|^2_{L^2(A\cup B)} + (|A|/2)\,\|f-f_{A\cup B}\|^2_{L^2(A\cup B)}\\
&= \operatorname{osc}_\ell(b)^2.
\end{aligned}$$

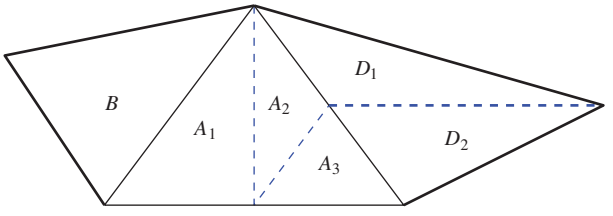

Figure 3. The element $A\in\mathcal{T}_\ell$ is refined by two bisections. It has two neighbouring elements B, $D\in\mathcal{T}_\ell$, whereas the third edge is on the boundary.

Next, we consider $d := A \cap D \in \mathcal{E}_\ell$. We have

$$o_\ell(d|D)^2 = (|A|/4 + |D|/2)\,\|f - f_{A_2\cup D_1}\|^2_{L^2(D_1)} + (|A|/4 + |D|/2)\,\|f - f_{A_3\cup D_2}\|^2_{L^2(D_2)},$$

$$o_\ell(d|A)^2 = (|D|/2 + |A|/4)\,\|f - f_{A_2\cup D_1}\|^2_{L^2(A_2)} + (|D|/2 + |A|/4)\,\|f - f_{A_3\cup D_2}\|^2_{L^2(A_3)} + (|A|/2)\,\|f - f_A\|^2_{L^2(A)}.$$

This implies

$$\begin{aligned} o_\ell(d|A)^2 + o_\ell(d|D)^2 &= (|A|/4+|D|/2)\,\|f-f_{A_2\cup D_1}\|^2_{L^2(A_2\cup D_1)} \\ &\quad + (|A|/4+|D|/2)\,\|f-f_{A_3\cup D_2}\|^2_{L^2(A_3\cup D_2)} + (|A|/2)\,\|f-f_A\|^2_{L^2(A)} \\ &\le (|A|/4+|D|/2)\,\|f-f_{A\cup D}\|^2_{L^2(A\cup D)} + (|A|/2)\,\|f-f_{A\cup D}\|^2_{L^2(A)} \\ &\le \frac{3}{4}\operatorname{osc}_\ell(d)^2. \end{aligned}$$

Finally, we consider the boundary edge $c := A \cap \Gamma \in \mathcal{E}_{\ell,\Gamma}$. In this case, there holds

$$o_\ell(c|A)^2 = (|A|/2)\,\|f\|^2_{L^2(A_1)} + (|A|/4)\,\|f\|^2_{L^2(A_3)} + (|A|/4)\,\|f-f_A\|^2_{L^2(A)} \le \frac{3}{4}\operatorname{osc}_\ell(c)^2,$$

and we also observe the contraction property.

Having obtained (21)–(22), we may proceed as follows: we note that (20) provides

$$\begin{aligned} \sum_{E\in\mathcal{E}^\star_{\ell+1}} \operatorname{osc}_{\ell+1}(E)^2 = \sum_{T\in\mathcal{T}_\ell} \sum_{\substack{E\in\mathcal{E}^\star_{\ell+1}\\ |T\cap\Omega_{\ell+1,E}|>0}} \operatorname{osc}_{\ell+1}(E|T)^2 &\le \sum_{T\in\mathcal{T}_\ell} \sum_{\substack{E\in\mathcal{E}^\star_\ell\\ E\subset\partial T}} o_\ell(E|T)^2 \\ &= \sum_{E\in\mathcal{E}^\star_\ell} \sum_{\substack{T\in\mathcal{T}_\ell\\ T\subset\Omega_{\ell,E}}} o_\ell(E|T)^2. \end{aligned}$$

Therefore, (21)–(22) show

$$\begin{aligned} \sum_{E\in\mathcal{E}^\star_{\ell+1}} \operatorname{osc}_{\ell+1}(E)^2 &\le \sum_{E\in\mathcal{E}^\star_\ell\cap\mathcal{E}^\star_{\ell+1}} \operatorname{osc}_\ell(E)^2 + \frac{3}{4}\sum_{E\in\mathcal{E}^\star_\ell\setminus\mathcal{E}^\star_{\ell+1}} \operatorname{osc}_\ell(E)^2 \\ &= \sum_{E\in\mathcal{E}^\star_\ell} \operatorname{osc}_\ell(E)^2 - \frac{1}{4}\sum_{E\in\mathcal{E}^\star_\ell\setminus\mathcal{E}^\star_{\ell+1}} \operatorname{osc}_\ell(E)^2 \end{aligned}$$

and conclude the proof. ■

Proof of Proposition 3.1 First, the triangle inequality in the sequence space ℓ_2 proves

$$\begin{aligned} \eta_{\ell+1} &= \left(\operatorname{osc}^2_{\ell+1} + \sum_{E'\in\mathcal{E}_{\ell+1}} h_{E'}\,\|[\partial_n U_{\ell+1}]\|^2_{L^2(E')}\right)^{1/2} \\ &\le \left(\operatorname{osc}^2_{\ell+1} + \sum_{E'\in\mathcal{E}_{\ell+1}} h_{E'}\,\|[\partial_n U_\ell]\|^2_{L^2(E')}\right)^{1/2} + \left(\sum_{E'\in\mathcal{E}_{\ell+1}} h_{E'}\,\|[\partial_n(U_{\ell+1}-U_\ell)]\|^2_{L^2(E')}\right)^{1/2}. \end{aligned}$$

In particular, the Young inequality yields for arbitrary $\delta > 0$

$$\eta_{\ell+1}^2 \le (1+\delta)\left(\operatorname{osc}_{\ell+1}^2 + \sum_{E' \in \mathcal{E}_{\ell+1}} h_{E'} \, \|[\partial_n U_\ell]\|_{L^2(E')}^2\right) + (1+\delta^{-1}) \sum_{E' \in \mathcal{E}_{\ell+1}} h_{E'} \, \|[\partial_n (U_{\ell+1} - U_\ell)]\|_{L^2(E')}^2. \tag{23}$$

Second, recall that $\mathcal{E}_\ell^\star \backslash \mathcal{E}_{\ell+1}^\star \supseteq \mathcal{M}_\ell$. Using the estimates (18) and (19), we thus see

$$\begin{aligned}
&\operatorname{osc}_{\ell+1}^2 + \sum_{E' \in \mathcal{E}_{\ell+1}} h_{E'} \, \|[\partial_n U_\ell]\|_{L^2(E')}^2 \\
&\quad \le \operatorname{osc}_\ell^2 + \sum_{E \in \mathcal{E}_\ell} h_E \, \|[\partial_n U_\ell]\|_{L^2(E)}^2 - \frac{1}{4} \sum_{E \in \mathcal{E}_\ell^\star \backslash \mathcal{E}_{\ell+1}^\star} \operatorname{osc}_\ell(E)^2 - \frac{1}{2} \sum_{E \in \mathcal{E}_\ell \cap \mathcal{M}_\ell} h_E \, \|[\partial_n U_\ell]\|_{L^2(E)}^2 \\
&\quad \le \eta_\ell^2 - \frac{1}{4} \left(\sum_{E \in \mathcal{M}_\ell} \operatorname{osc}_\ell(E)^2 + \sum_{E \in \mathcal{E}_\ell \cap \mathcal{M}_\ell} h_E \, \|[\partial_n U_\ell]\|_{L^2(E)}^2 \right).
\end{aligned}$$

Third, the Dörfler marking (16) is used to obtain

$$\operatorname{osc}_{\ell+1}^2 + \sum_{E' \in \mathcal{E}_{\ell+1}} h_{E'} \, \|[\partial_n U_\ell]\|_{L^2(E')}^2 \le \eta_\ell^2 - \frac{1}{4} \sum_{E \in \mathcal{M}_\ell} \eta_\ell(E)^2 \le (1 - \theta/4) \eta_\ell^2.$$

Fourth, according to uniform shape regularity of the generated family $(\mathcal{T}_\ell)_{\ell \in \mathbb{N}}$, there holds

$$\sum_{E' \in \mathcal{E}_{\ell+1}} h_{E'} \, \|[\partial_n (U_{\ell+1} - U_\ell)]\|_{L^2(E')}^2 \lesssim \|\nabla (U_{\ell+1} - U_\ell)\|_{L^2(\Omega)}^2 = \|\!| U_{\ell+1} - U_\ell |\!\|^2.$$

Plugging the last two estimates into (23), we prove (17), where we finally choose $\delta > 0$ sufficiently small to guarantee $q := (1+\delta)(1-\theta/4) < 1$. ∎

Remark 1 Clearly, Lemma 3.2 also holds if certain elements $T \in \mathcal{T}_\ell$ are refined by five bisections, as is done in [18], or by the so-called red-refinement. We refer to [1, Chap. 4] for details on different local mesh-refinements.

The same holds for Lemma 3.3 as well. In case of bisec_5-refinement this is easily seen as follows: we theoretically build an intermediate mesh $\mathcal{T}_{\ell+1/2}$, where elements marked for bisec_5 are only refined by three bisections. Then, Lemma 3.3 applies for the refinement from $\mathcal{T}_\ell$ to $\mathcal{T}_{\ell+1/2}$. To finally obtain $\mathcal{T}_{\ell+1}$, certain elements $T' \in \mathcal{T}_{\ell+1/2}$ have to be refined by one bisection. Note that this guarantees $\mathcal{E}_\ell^\star \backslash \mathcal{E}_{\ell+1/2}^\star = \mathcal{E}_\ell^\star \backslash \mathcal{E}_{\ell+1}^\star$ since only certain interior edges $E' \in \mathcal{E}_{\ell+1/2} \backslash \mathcal{E}_\ell$ are effected. Since (19) states, in particular, monotone decay of the oscillations, we conclude

$$\operatorname{osc}_{\ell+1}^2 \le \operatorname{osc}_{\ell+1/2}^2 \le \sum_{E \in \mathcal{E}_\ell^\star} \operatorname{osc}_\ell(E)^2 - \frac{1}{4} \sum_{E \in \mathcal{E}_\ell^\star \backslash \mathcal{E}_{\ell+1}^\star} \operatorname{osc}_\ell(E)^2,$$

where $\operatorname{osc}_{\ell+1/2}$ denotes the oscillation term associated with the only theoretically constructed mesh $\mathcal{T}_{\ell+1/2}$.

Finally, if certain elements of $\mathcal{T}_\ell$ are refined by red-refinement, the proof of (19) is obtained by similar calculations as in the proof of Lemma 3.3. We refer to [24] for details.

3.2. *Convergent adaptive algorithm*

In this section, we formally state our version of the adaptive algorithm and prove that it generates a sequence of discrete solutions U_ℓ which converge to the continuous minimizer u.

Algorithm 1 Fix $0 < \theta < 1$ and let $\mathcal{T}_\ell$ with $\ell = 0$ be the initial triangulation. For each $\ell = 0, 1, 2, \ldots$, do:

(i) Compute discrete solution $U_\ell \in \mathcal{A}_\ell := \mathcal{A} \cap \mathcal{S}^1(\mathcal{T}_\ell)$
(ii) Compute indicators $\eta_\ell(E)$ for all $E \in \mathcal{E}_\ell^\star$.
(iii) Determine set $\mathcal{M}_\ell \subseteq \mathcal{E}_\ell^\star$ which satisfies (16).
(iv) Mark all edges $E \in \mathcal{M}_\ell$ for refinement.
(v) Obtain new mesh $\mathcal{T}_{\ell+1}$ by newest vertex bisection and increase counter $\ell \mapsto \ell + 1$.

THEOREM 3.4 *Algorithm* 1 *guarantees that the combined error quantity*

$$\Delta_\ell := \mathcal{J}(U_\ell) - \mathcal{J}(u) + \gamma\, \eta_\ell^2 \tag{24}$$

satisfies the contraction property

$$\Delta_{\ell+1} \le \kappa\, \Delta_\ell \quad \text{for all } \ell \in \mathbb{N}. \tag{25}$$

The constants $0 < \gamma$, $\kappa < 1$ *depend only on the parameter* θ *and the shape of the elements in* $\mathcal{T}_0$. *In particular, there holds* $\lim_{\ell\to\infty} \mathcal{J}(U_\ell) = \mathcal{J}(u)$ *as well as* $\lim_{\ell\to\infty} |||u - U_\ell||| = 0 = \lim_{\ell\to\infty} \eta_\ell$.

Proof According to Proposition 3.1, we have

$$\eta_{\ell+1}^2 \le q\, \eta_\ell^2 + C_2\, |||U_{\ell+1} - U_\ell|||^2$$

with certain constants $0 < q < 1$ and $C_2 > 0$. Therefore,

$$\begin{aligned}\Delta_{\ell+1} &= \mathcal{J}(U_\ell) - \mathcal{J}(u) + \gamma\, \eta_{\ell+1}^2 - (\mathcal{J}(U_\ell) - \mathcal{J}(U_{\ell+1})) \\ &\le \mathcal{J}(U_\ell) - \mathcal{J}(u) + \gamma q\, \eta_\ell^2 + \gamma C_2\, |||U_{\ell+1} - U_\ell|||^2 - (\mathcal{J}(U_\ell) - \mathcal{J}(U_{\ell+1})).\end{aligned}$$

Using the variational inequality (9) applied for $U_{\ell+1}$, we proceed as in the proof of Proposition 2.2 to see

$$\frac{1}{2}\, |||U_{\ell+1} - U_\ell|||^2 \le \mathcal{J}(U_\ell) - \mathcal{J}(U_{\ell+1}).$$

Choosing γ sufficiently small to guarantee $\gamma C_2 - 1/2 \le 0$, we then obtain

$$\Delta_{\ell+1} \le \mathcal{J}(U_\ell) - \mathcal{J}(u) + \gamma q\, \eta_\ell^2 + (\gamma C_2 - 1/2)\, |||U_{\ell+1} - U_\ell|||^2 \le \mathcal{J}(U_\ell) - \mathcal{J}(u) + \gamma q\, \eta_\ell^2.$$

According to Proposition 2.2, there holds

$$C_1^{-1}\, (\mathcal{J}(U_\ell) - \mathcal{J}(u)) \le \eta_\ell^2.$$

For $\varepsilon > 0$, we thus observe

$$\mathcal{J}(U_\ell) - \mathcal{J}(u) + \gamma q\, \eta_\ell^2 \le (1 - \gamma\varepsilon C_1^{-1})(\mathcal{J}(U_\ell) - \mathcal{J}(u)) + \gamma(q + \varepsilon)\eta_\ell^2 \le \kappa\, \Delta_\ell \tag{26}$$

with $\kappa := \max\{1 - \gamma\varepsilon C_2^{-1}, q + \varepsilon\}$. Since $q < 1$, we may choose $\varepsilon > 0$ sufficiently small to guarantee $q + \varepsilon < 1$. This choice leads to $\kappa < 1$, and we finally end up with (25). By induction, this implies

$$\lim_{\ell\to\infty} \Delta_\ell = 0, \quad \text{whence} \quad \lim_{\ell\to\infty} \mathcal{J}(U_\ell) = \mathcal{J}(u) \text{ and } \lim_{\ell\to\infty} \eta_\ell = 0.$$

With reliability $|||u - U_\ell||| \lesssim \eta_\ell$, we thus conclude the proof. ■

In [18], the weighting $h_T^2 = \operatorname{diam}(T)^2$ instead of $|T|$ is used in the definition (14) of $\operatorname{osc}_\ell(E)$, i.e.

$$\widetilde{\eta}_\ell^2 := \sum_{E\in\mathcal{E}_\ell} \big(\varrho_\ell(E)^2 + \operatorname{osc}_\ell(E)^2\big) + \sum_{E\in\mathcal{E}_{\ell,\Gamma}} \widetilde{\operatorname{osc}}_\ell(E)^2, \tag{27}$$

where

$$\widetilde{\operatorname{osc}}_\ell(E)^2 = h_T^2 \,\|f\|_{L^2(T)}^2 \quad \text{for } E\in\mathcal{E}_{\ell,\Gamma} \tag{28}$$

and $T\in\mathcal{T}_\ell$ is the unique element with $E = \partial T \cap \Gamma$. Note that this definition does not necessarily yield a contraction $h_{T'} < h_T$ if an edge $E\in\mathcal{E}_{\ell,\Gamma}\cap\mathcal{M}_\ell$ is refined and $T'\in\mathcal{T}_{\ell+1}$ is one of the resulting sons of T. Nevertheless, $\widetilde{\eta}_\ell$ leads to a convergent adaptive FEM in the sense of Theorem 3.4.

COROLLARY 3.5 *Suppose that $\widetilde{\eta}_\ell$ instead of η_ℓ is used in Algorithm* 1 *for marking. Then, the modified algorithm still guarantees the contraction property* (25). *In particular, there holds* $\lim_{\ell\to\infty} \mathcal{J}(U_\ell) = \mathcal{J}(u)$ *as well as* $\lim_{\ell\to\infty} |||u - U_\ell||| = 0 = \lim_{\ell\to\infty} \widetilde{\eta}_\ell$.

Proof Note that there holds

$$\operatorname{osc}_\ell(E) \le \widetilde{\operatorname{osc}}_\ell(E) \le C_3 \operatorname{osc}_\ell(E) \quad \text{for all } E\in\mathcal{E}_{\ell,\Gamma} \tag{29}$$

with some constant $C_3 \ge 1$ which depends only on the shape regularity of the mesh $\mathcal{T}_\ell$. Since newest vertex bisection leads to uniformly shape regular meshes, C_3 may be chosen independently of ℓ. The Dörfler marking (16) for $\widetilde{\eta}_\ell$ thus implies

$$\begin{aligned}\theta\,\eta_\ell \le \theta\,\widetilde{\eta}_\ell &\le \sum_{E\in\mathcal{E}_\ell\cap\mathcal{M}_\ell} \big(\varrho_\ell(E)^2 + \operatorname{osc}_\ell(E)^2\big) + \sum_{E\in\mathcal{E}_{\ell,\Gamma}\cap\mathcal{M}_\ell} \widetilde{\operatorname{osc}}_\ell(E)^2 \\ &\le C_3 \left(\sum_{E\in\mathcal{E}_\ell\cap\mathcal{M}_\ell} \big(\varrho_\ell(E)^2 + \operatorname{osc}_\ell(E)^2\big) + \sum_{E\in\mathcal{E}_{\ell,\Gamma}\cap\mathcal{M}_\ell} \operatorname{osc}_\ell(E)^2 \right).\end{aligned}$$

Put differently, the set $\mathcal{M}_\ell$ satisfies the Dörfler marking (16) for $(\theta, \widetilde{\eta}_\ell)$ as well as the Dörfler marking (16) for $(\widetilde{\theta}, \eta_\ell)$, where $\widetilde{\theta} = \theta/C_3 \in (0,1)$. Therefore, Theorem 3.4 applies and (25) holds. In particular, $\lim_{\ell\to\infty} \eta_\ell = 0$ and the equivalence (29) also concludes $\lim_{\ell\to\infty} \widetilde{\eta}_\ell = 0$. ■

Remark 2 The estimator reduction (17) already implies convergence $\lim_\ell \eta_\ell = 0$, whence $\lim_\ell \mathcal{J}(U_\ell) = \mathcal{J}(u)$ as well as $\lim_\ell |||u - U_\ell||| = 0$ according to Proposition 2.2. To see this, it remains to verify that the obstacle problem leads to *a priori convergence* $\lim_\ell U_\ell = u_\infty$ with a certain limit $u_\infty \in \mathcal{H}$. For linear problems, such a

result is found in [25–27], and we refer to [24, Lemma 3.3.8] for the proof of the *a priori* convergence in our non-linear setting. Then, (17) takes the form

$$\eta_{\ell+1}^2 \leq q\,\eta_\ell^2 + \alpha_\ell$$

with the zero sequence $\alpha_\ell = C_2\ |||U_{\ell+1} - U_\ell|||^2 \geq 0$. Therefore, elementary calculus concludes $\lim_\ell \eta_\ell = 0$ (cf [25]). We stress that, contrary to [27], the estimator reduction concept from [25] avoids any use of discrete efficiency. It is only based on the precise definition of the error estimator, a uniform decay of the mesh-width locally on marked elements, and the observation that any kind of mesh-refinement will lead to a convergent sequence of discrete solutions. We stress, however, that the convergence results in Theorem 3.4 and Corollary 3.5 are stronger since they include even a contraction of some error quantity $\Delta_\ell \geq \varepsilon_\ell = \mathcal{J}(U_\ell) - \mathcal{J}(u)$.

3.3. *Convergence analysis for the adaptive algorithm from [18]*

In this section, we aim to comment briefly on the adaptive algorithm in [18] and improve their convergence result in several aspects.

Algorithm 2 Fix $0 < \theta, \vartheta < 1$ and let $\mathcal{T}_\ell$ with $\ell = 0$ be the initial triangulation. For each $\ell = 0, 1, 2, \ldots$, do:

(i) Compute discrete solution $U_\ell \in \mathcal{A}_\ell := \mathcal{A} \cap \mathcal{S}^1(\mathcal{T}_\ell)$
(ii) Compute indicators $\varrho_\ell(E)^2$ as well as oscillation terms $\mathrm{osc}_\ell(E)$ for all $E \in \mathcal{E}_\ell^\star$.
(iii) Determine set $\mathcal{M}_\ell \subseteq \mathcal{E}_\ell$ which satisfies

$$\theta \sum_{E\in\mathcal{E}_\ell} \varrho_\ell(E)^2 \leq \sum_{E\in\mathcal{M}_\ell} \varrho_\ell(E)^2. \tag{30}$$

(iv) Mark all edges $E \in \mathcal{M}_\ell$ for refinement and obtain intermediate mesh $\mathcal{T}_{\ell+1/2}$ by newest vertex bisection of $\mathcal{T}_\ell$.
(v) Refine additional elements of $\mathcal{T}_{\ell+1/2}$ and update $\mathcal{T}_{\ell+1/2}$ until the corresponding oscillations satisfy $\mathrm{osc}_{\ell+1/2} \leq \vartheta\ \mathrm{osc}_\ell$.
(vi) Finally, set $\mathcal{T}_{\ell+1} := \mathcal{T}_{\ell+1/2}$ and increase counter $\ell \mapsto \ell + 1$.

In Braess et al. [18], the authors do not give further information on step (v) besides their choice $\theta = \vartheta$. In particular, it is not obvious how many levels of refinement have to be done until $\mathrm{osc}_{\ell+1} \leq \vartheta\ \mathrm{osc}_\ell$ is satisfied. In the following, we comment on a practical realization of (v) and derive a convergence result similar to Theorem 3.4. Our recommendation reads as follows:

(v.a) If $\mathrm{osc}_{\ell+1/2}^2 \leq (1 - \theta/4)\mathrm{osc}_\ell^2$, define $\mathcal{T}_{\ell+1} := \mathcal{T}_{\ell+1/2}$
(v.b) Otherwise determine $\mathcal{M}_{\ell+1/2} \subseteq \mathcal{E}_{\ell+1/2}^\star$ such that

$$\theta\,\mathrm{osc}_{\ell+1/2}^2 \leq \sum_{E\in\mathcal{M}_{\ell+1/2}} \mathrm{osc}_{\ell+1/2}(E)^2, \tag{31}$$

(v.c) mark all edges $E \in \mathcal{M}_{\ell+1/2}$ for refinement,
(v.d) and obtain new mesh $\mathcal{T}_{\ell+1}$ by newest vertex bisection.

We first prove that this part guarantees contraction of the data oscillations.

LEMMA 3.6 *The proposed realization of step* (v) *in Algorithm* 2 *guarantees* $\operatorname{osc}_{\ell+1} \le \vartheta \operatorname{osc}_\ell$ *with* $\vartheta = (1-\theta/4)^{1/2}$.

Proof We may assume that $\operatorname{osc}_{\ell+1/2}^2 > (1-\theta/4)\operatorname{osc}_\ell^2$ since otherwise $\operatorname{osc}_{\ell+1/2} = \operatorname{osc}_{\ell+1}$ by definition. Using Lemma 3.3 and arguing as in the proof of Proposition 3.1 (but only for the oscillation terms), we see that the marking criterion (31) guarantees $\operatorname{osc}_{\ell+1}^2 \le (1-\theta/4)\operatorname{osc}_{\ell+1/2}^2$. Since $\mathcal{T}_{\ell+1/2}$ is a refinement of $\mathcal{T}_\ell$, the monotonicity $\operatorname{osc}_{\ell+1/2} \le \operatorname{osc}_\ell$ of the edge oscillations concludes the proof. ■

Next, we prove an estimator reduction similar to Proposition 3.1.

PROPOSITION 3.7 *The extended Algorithm* 2 *from* [18] *guarantees*

$$\eta_{\ell+1}^2 \le q\,\eta_\ell^2 + C_4\Big(\big|\!\big|\!\big| U_{\ell+1/2} - U_\ell \big|\!\big|\!\big|^2 + \big|\!\big|\!\big| U_{\ell+1} - U_{\ell+1/2} \big|\!\big|\!\big|^2\Big), \quad \text{for all } \ell \in \mathbb{N}, \tag{32}$$

with constants $q \in (0,1)$ *and* $C_4 > 0$ *which depend only on* $\theta \in (0,1)$ *and the shape of the elements in* $\mathcal{T}_0$.

Proof Note that $\mathcal{T}_{\ell+1}$ is a refinement of $\mathcal{T}_{\ell+1/2}$, and $\mathcal{T}_{\ell+1/2}$ is a refinement of $\mathcal{T}_\ell$. Arguing as in the proof of Proposition 3.1 (but only for the edge jumps), we see that the modified marking criterion (30) yields

$$\begin{aligned}\sum_{E'' \in \mathcal{E}_{\ell+1}} \varrho_{\ell+1}(E'')^2 &\le (1+\delta) \sum_{E' \in \mathcal{E}_{\ell+1/2}} \varrho_{\ell+1/2}(E')^2 + C(1+\delta^{-1}) \big|\!\big|\!\big| U_{\ell+1} - U_{\ell+1/2} \big|\!\big|\!\big|^2 \\ &\le (1+\delta)^2(1-\theta/2) \sum_{E \in \mathcal{E}_\ell} \varrho_\ell(E)^2 + C(1+\delta^{-1}) \\ &\quad \times \Big(\big|\!\big|\!\big| U_{\ell+1} - U_{\ell+1/2} \big|\!\big|\!\big|^2 + \big|\!\big|\!\big| U_{\ell+1/2} - U_\ell \big|\!\big|\!\big|^2 \Big),\end{aligned}$$

for all $\delta > 0$. As above, the constant $C > 0$ stems from inverse-type estimates and depends only on the uniform shape regularity of the meshes involved. In view of the contraction from Lemma 3.6, we choose $\delta > 0$ sufficiently small such that $(1+\delta)^2(1-\theta/2) \le (1-\theta/4)$. Adding the estimate of Lemma 3.6, we conclude the proof with $q = (1-\theta/4)$. ■

Finally, we argue as in the proof of Theorem 3.4 to obtain the following convergence result whose proof is omitted for brevity. We stress that our result is superior to the convergence result from [18] for several reasons: First, we only need one bisection instead of five per refined element. Second, our recommendation of $\vartheta = (1-\theta/4)^{1/2}$ satisfies $\vartheta \ge \theta$ for practical choices of θ, namely $\theta < 0.88$. Third, our modification of their algorithm guarantees that at most one additional step of newest vertex bisection has to be performed to guarantee contraction of the oscillations.

THEOREM 3.8 *The extended Algorithm* 2 *from* [18] *guarantees*

$$\Delta_{\ell+1} \le \kappa\,\Delta_\ell \quad \text{with} \quad \Delta_\ell := \mathcal{J}(U_\ell) - \mathcal{J}(u) + \gamma\,\eta_\ell^2 \quad \text{for all } \ell \in \mathbb{N}. \tag{33}$$

The constants $0 < \gamma,\ \kappa < 1$ *depend only on the parameter* θ *and the shape of the elements in* $\mathcal{T}_0$. *In particular, there holds* $\lim_{\ell\to\infty} \mathcal{J}(U_\ell) = \mathcal{J}(u)$ *as well as* $\lim_{\ell\to\infty} |\!|\!| u - U_\ell |\!|\!| = 0 = \lim_{\ell\to\infty} \eta_\ell$.

4. Numerical experiment

In this section, we consider a numerical experiment from [18]. The conforming and shape regular mesh is adaptively generated by Algorithm 1. For the solution of the discrete obstacle problem at each level, the primal-dual active set strategy from [28] has been used. For the initial mesh $\mathcal{T}_0$, we choose $(U_0^{(0)}, \lambda_0^{(0)}) \equiv (0,0)$ for the primal dual pair as initial guesses for the iterative solver. For $\mathcal{T}_\ell$, we choose the prolongated discrete solutions associated with the previous mesh, i.e. $U_\ell^{(0)} := U_{\ell-1}$ as well as $\lambda_\ell^{(0)} := \lambda_{\ell-1}$. We stop the iterative solver if the difference of two consecutive solutions satisfies

$$\left\| U_\ell^{(j)} - U_\ell^{(j-1)} \right\| \leq \tau\, N^{-1/2} \tag{34}$$

for some tolerance $\tau > 0$, where $N = \#\mathcal{T}_\ell$ denotes the number of elements. We then define our discrete solution at $\mathcal{T}_\ell$ by $U_\ell := U_\ell^{(j)}$ and $\lambda_\ell := \lambda_\ell^{(j)}$.

While the numerical results are quite similar to those in [18], we stress that our approach theoretically includes the data oscillations into the estimator η_ℓ.

We consider the obstacle problem with constant obstacle $\chi \equiv 0$ on the L-shaped domain $\Omega := (-2,\ 2)^2 \setminus\ [0,\ 2) \times (-2,\ 0]$. The right-hand side is given in polar coordinates by

$$f(r,\varphi) := -\, r^{2/3} \sin(2\varphi/3)\big(\gamma_1'(r)/r + \gamma_1''(r)\big) - \frac{4}{3}\, r^{-1/3}\gamma_1'(r)\sin(2\varphi/3) - \gamma_2(r), \tag{35}$$

where $(\cdot)'$ denotes the radial derivative $\mathrm{d}/\mathrm{d}r$. Moreover, $\bar{r} := 2(r - 1/4)$ and

$$\gamma_1(r) = \begin{cases} 1, & \bar{r} < 0, \\ -6\bar{r}^5 + 15\bar{r}^4 - 10\bar{r}^3 + 1, & 0 \leq \bar{r} < 1, \\ 0, & \bar{r} \geq 1, \end{cases}$$

$$\gamma_2(r) = \begin{cases} 0, & r \leq 5/4, \\ 1, & \text{else.} \end{cases}$$

Then, the exact solution reads in polar coordinates

$$u(r,\varphi) = r^{2/3}\gamma_1(r)\sin(2\varphi/3) \tag{36}$$

and exhibits a corner singularity at the origin. We compare uniform and adaptive mesh-refinement, where we vary the adaptivity parameter $\theta \in \{0.2, 0.4, 0.6, 0.8\}$ in Algorithm 1. The quantities of interest are the energy error

$$\varepsilon_\ell = \mathcal{J}(U_\ell) - \mathcal{J}(u), \tag{37}$$

as well as the error estimator η_ℓ from (11) which includes oscillations and edge jumps. Since the oscillations are, however, expected to be of higher order, the values of osc_ℓ are explicitly given.

In Figure 4, we plot $\sqrt{\varepsilon_\ell}$, η_ℓ and osc_ℓ over the number $N = \#\mathcal{T}_\ell$ of elements for uniform and adaptive mesh-refinement with $\theta = 0.6$. Uniform mesh-refinement leads to a suboptimal convergence behaviour $\sqrt{\varepsilon_\ell} \approx \mathcal{O}(N^{-5/12})$ with respect to the number $N = \#\mathcal{T}_\ell$ of elements. Contrary, adaptive mesh-refinement regains the optimal order of convergence $\sqrt{\varepsilon_\ell} = \mathcal{O}(N^{-1/2})$. We stress that the given data are smooth so that uniform as well as adaptive mesh-refinement leads to $\mathrm{osc}_\ell = \mathcal{O}(N^{-1})$, which

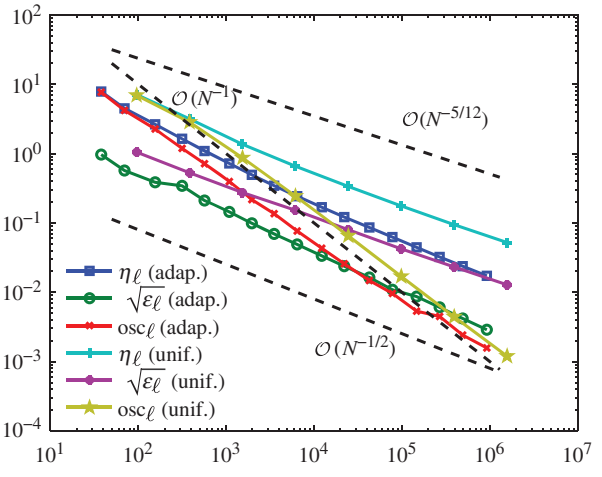

Figure 4. Numerical results for uniform and adaptive mesh-refinement with $\theta = 0.6$, where $\varepsilon_\ell = \mathcal{J}(U_\ell) - \mathcal{J}(u)$, η_ℓ and osc$_\ell$ are plotted over the number $N = \#\mathcal{T}_\ell$ of elements.

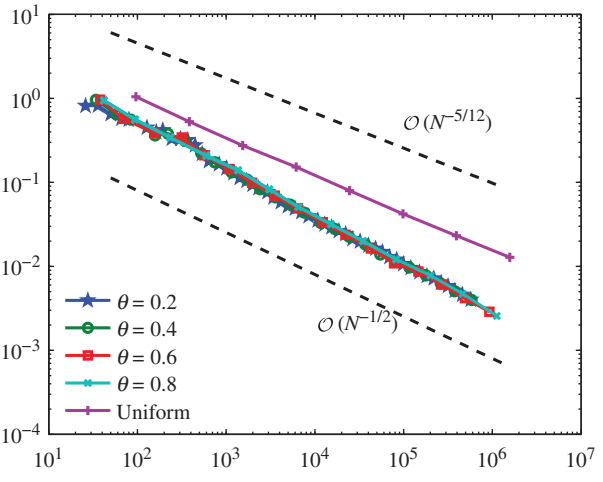

Figure 5. Numerical results for $\sqrt{\varepsilon_\ell}$ for uniform and adaptive mesh-refinement with $\theta \in \{0.2, 0.4, 0.6, 0.8\}$, plotted over the number $N = \#\mathcal{T}_\ell$ of elements.

corresponds to second-order convergence with respect to a uniform mesh-width. For both mesh-refinements, we see that the curves of η_ℓ and $\sqrt{\varepsilon_\ell}$ are parallel. This experimentally confirms the reliability of η_ℓ from Proposition 2.2 and indicates that η_ℓ is also efficient.

Figure 5 provides the experimental comparison for different values of $\theta \in \{0.2, 0.4, 0.6, 0.8\}$. We see that each choice of θ leads to optimal order of convergence and that the corresponding curves essentially coincide. Since achievement of a prescribed precision takes much longer with uniform refinement, the benefits of adaptive refinement are clearly visible. Additionally, we stress that also the convergence rate itself is improved.

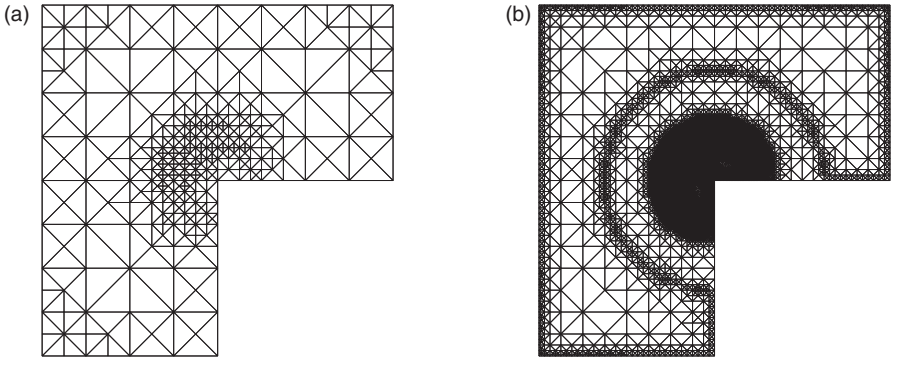

Figure 6. Adaptively generated meshes $\mathcal{T}_5$ (a) and $\mathcal{T}_{11}$ (b) with $N = 568$ and $N = 22140$ elements, respectively, for $\theta = 0.6$.

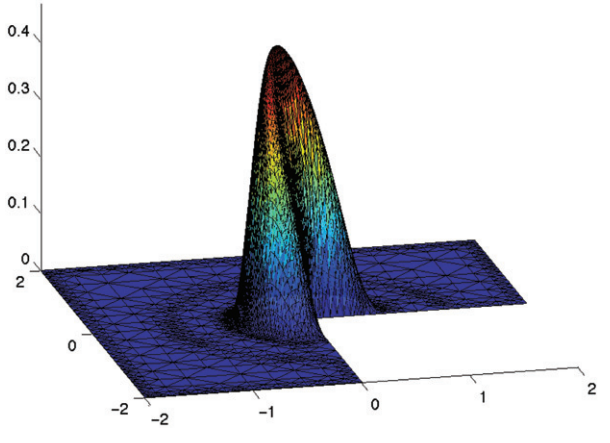

Figure 7. Galerkin solution U_8 on adaptively generated mesh $\mathcal{T}_8$ with $N = 3524$ elements for $\theta = 0.6$.

Figure 6 displays the adaptively generated meshes $\mathcal{T}_5$ and $\mathcal{T}_{11}$, respectively for $\theta = 0.6$. As expected, refinement is basically restricted to the inactive zone. Due to the data oscillation terms in the estimator η_ℓ, we also observe certain refinement within the active zone. Note that the corresponding figures in [18] do not show any refinement inside the active zone. We stress, however, that those figures are somewhat misleading in the following sense: the right-hand side f is non-zero along the boundary in this example. Therefore, the contraction of the overall oscillations (as it is postulated by [18]) can only be achieved if (sooner or later) refinements take place also within the active zone. The algorithm from [18] will thus eventually lead to the very same refinement along the boundary that we observe here.

Finally, the numerical solutions after eight steps of refinement is shown in Figure 7.

Acknowledgements

The authors acknowledge support of the Viennese Science and Technology Fund (WWTF) through the research project MA09–029 *Micromagnetic Simulation and Computational Design*

of Future Devices. The second author (D.P.) acknowledges support of the Austrian Science Fund (FWF) through the project *Adaptive Boundary Element Method* under grant P21732.

References

[1] R. Verfürth, *A Review of a Posteriori Error Estimation and Adaptive Mesh-refinement Techniques*, Wiley-Teubner, New York, 1996.
[2] M. Ainsworth and T. Oden, *A Posteriori Error Estimation in Finite Element Analysis*, Wiley-Interscience, New-York, 2000.
[3] M. Ainsworth, C. Lee, and T. Oden, *Local a posterori error estimators for variational inequalities*, Numer. Meth. Part. D. E. 9 (1993), pp. 23–33.
[4] D. Braess, *A posteriori error estimators for obstacle problems – Another look*, Numer. Math. 101 (2005), pp. 415–421.
[5] S. Bartels and C. Carstensen, *Averaging techniques yield reliable a posteriori finite element error control for obstacle problems*, Numer. Math. 99 (2004), pp. 225–249.
[6] Z. Chen and R. Nochetto, *Residual type a posteriori error estimates for elliptic obstacle problems*, Numer. Math. 84 (2000), pp. 527–548.
[7] C. Gräser, R. Kornhuber, A. Veeser, and Q. Zou, *Hierarchical error estimates for the energy functional in obstacle problems*, Numer. Math. 117 (2011), pp. 653–677.
[8] W. Liu and N. Yan, *A posteriori error estimates for a class of variational inequalities*, J. Sci. Comput. 15 (2000), pp. 361–393.
[9] R. Nochetto, K. Siebert, and A. Veeser, *Fully localized a posteriori error estimators and barrier sets for contact problems*, SIAM J. Numer. Anal. 42 (2005), pp. 2118–2135.
[10] K. Siebert and A. Veeser, *A uniliterally constrained quadratic minimization with adaptive finite elements*, SIAM. J. Optim. 18 (2007), pp. 260–289.
[11] A. Veeser, *Efficient and reliable a posteriori error estimators for elliptic obstacle problems*, SIAM J. Numer. Anal. 39 (2001), pp. 146–167.
[12] W. Dörfler, *A convergent adaptive algorithm for Poisson's equation*, SIAM J. Numer. Anal. 33 (1996), pp. 1106–1124.
[13] P. Morin, R. Nochetto, and K. Siebert, *Data oscillation and convergence of adaptive FEM*, SIAM. J. Numer. Anal. 18 (2000), pp. 466–488.
[14] A. Veeser, *Convergent adaptive finite elements for the nonlinear Laplacian*, Numer. Math. 92 (2002), pp. 743–770.
[15] C. Carstensen and R. Hoppe, *Convergence analysis of an adaptive edge finite element method for the 2D eddy current equations*, J. Numer. Math. 13 (2005), pp. 19–32.
[16] C. Carstensen and R. Hoppe, *Error reduction and convergence for an adaptive mixed finite element method*, Math. Comp. 75 (2006), pp. 1033–1042.
[17] C. Carstensen and R. Hoppe, *Convergence analysis of an adaptive nonconforming finite element method*, Numer. Math. 103 (2006), pp. 251–266.
[18] D. Braess, C. Carstensen, and R. Hoppe, *Convergence analysis of a conforming adaptive finite element method for an obstacle problem*, Numer. Math. 107 (2007), pp. 455–471.
[19] D. Braess, C. Carstensen, and R. Hoppe, *Error reduction in adaptive finite element approximations of elliptic obstacle problems*, J. Comput. Math. 27 (2009), pp. 148–169.
[20] R. Stevenson, *Optimality of standard adaptive finite element method*, Found. Comput. Math. 3 (2007), pp. 245–269.
[21] J. Cascon, C. Kreuzer, R. Nochetto, and K Siebert, *Quasi-optimal convergence rate for an adaptive finite element method*, SIAM J. Numer. Anal. 46 (2008), pp. 2524–2550.
[22] A. Friedman, *Variational Principles and Free-boundary Problems*, Wiley, New York, 1982.
[23] D. Kinderlehrer and G. Stampacchia, *An Introduction to Variational Inequalities*, Academic Press, New York, 1980.

[24] M. Page, *Schätzerreduktion und Konvergenz adaptiver FEM für Hindernisprobleme*, *Master thesis (in German)*, Institute for Analysis and Scientific Computing, Vienna University of Technology, Wien, 2010.
[25] M. Aurada, S. Ferraz-Leite, and D. Praetorius, *Estimator reduction and convergence of adaptive FEM and BEM*, ASC Report 27/2009, Institute for Analysis and Scientific Computing, Vienna University of Technology, Wien, 2009.
[26] C. Carstensen and D. Praetorius, *Convergence of adaptive boundary element methods*, ASC Report 15/2009, Institute for Analysis and Scientific Computing, Vienna University of Technology, Wien, 2009.
[27] P. Morin, K. Siebert, and A. Veeser, *A basic convergence result for conforming adaptive finite elements*, Math. Models Methods Appl. Sci. 18 (2008), pp. 707–737.
[28] M. Hintermüller, K. Ito, and K. Kunisch, *The primal-dual active set strategy as a semismooth newton method*, SIAM J. Optim. 13 (2003), pp. 865–888.